Supplementary Information

Appendix A: Real part of the polarization coefficient ($\mathrm{Re}[\tilde{f}_{CM}^{(2)}]$) for quadrupole

of T lymphocytes, B lymphocytes, granulocytes, monocytes, SkBr3, and A549
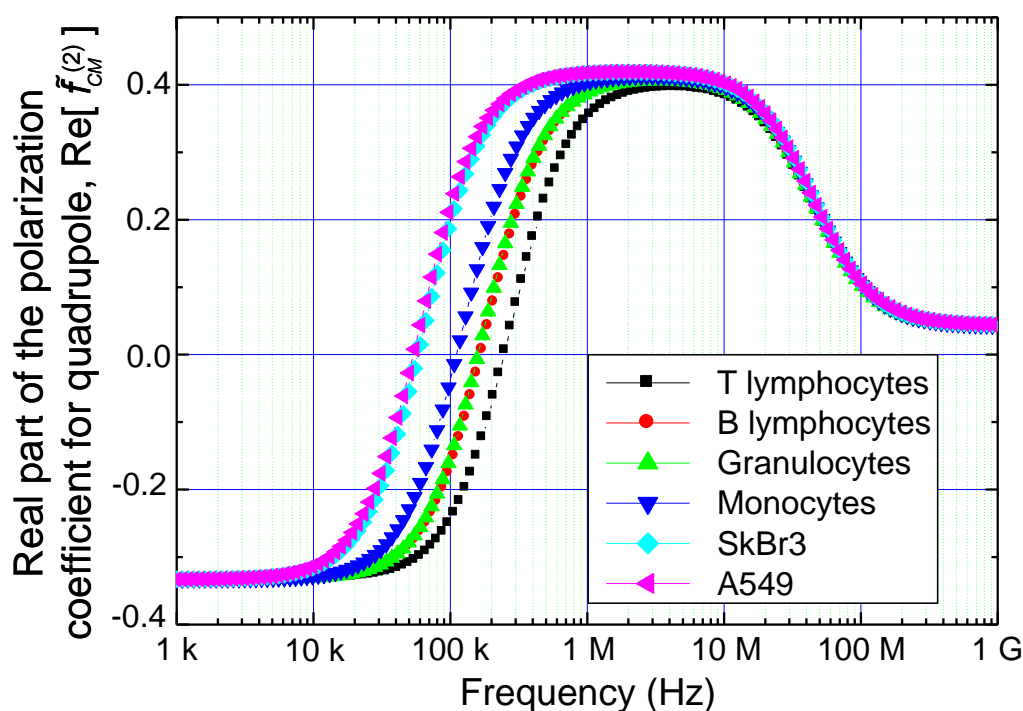
Fig. S1 Calculated real part of the polarization coefficient ($\mathrm{Re}[\tilde{f}_{CM}^{(2)}]$) for quadrupole of

human leukocyte subpopulations [T lymphocyte (—■—), B lymphocyte (—●—), granulocyte

(—▲—), and monocyte (—▼—)], and metastatic breast [SkBr3 (—◆—)] and lung [A549

(—◀—)] cancer cell lines, suspended in a 32.6 mS m^{-1} low-conductivity medium. The

measured size and dielectric properties of the cells (Table 1) were used for this calculation.

Appendix B: Point charge octupole model
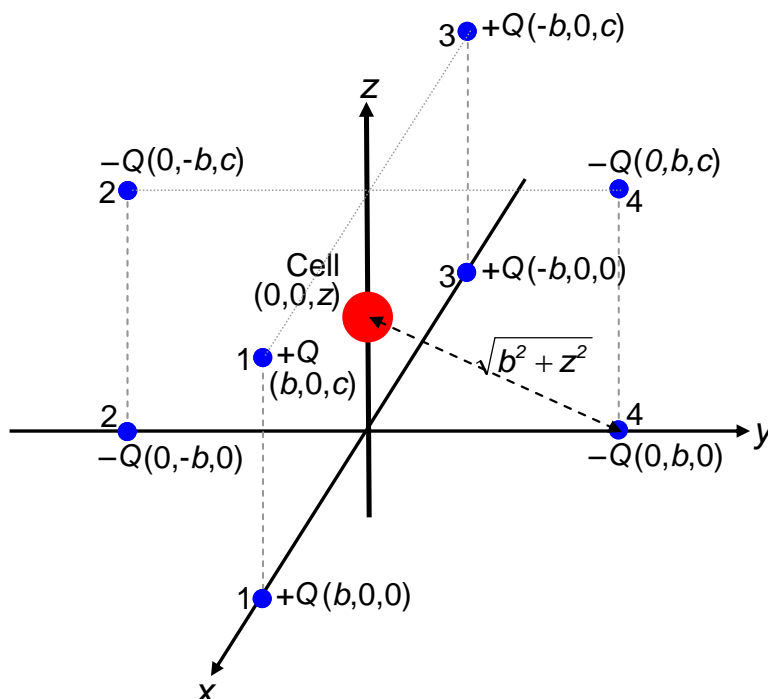
Fig. S2 A point charge octupole model showing the locations of the eight point charges $+Q$ at $(\pm b, 0, 0)$ and $(\pm b, 0, c)$ and $-Q$ at $(0, \pm b, 0)$ and $(0, \pm b, c)$. A cell of radius r is located on the central axis, the z-axis, of the octupole.

For the point charge octupole model (Fig. S2), if the radius of the cell, r, is much shorter than the distance between the center of the cell and the point charges on the bottom, $\sqrt{b^2 + z^2}$, the z-directional nQDEP force, acting on the cell on the central axis of the octupole, generated from the four point charges at $(\pm b, \pm b, 0)$ on the bottom can be calculated using Eq. (4). In the equation, the point charge, Q, is expressed as:

$$Q = 2\,C_{ele}V_{rms} = \sqrt{2}\,C_{ele}V_p \tag{S1}$$

2

where C_{ele} is the total sum of the mutual capacitances of an electrode with respect to oppositely polarized electrodes. V_{rms} and V_p are the root mean square voltage and the peak voltage of the nQDEP signal, respectively.

Using finite element analysis with commercially available software, ANSYS (ANSYS Inc.), C_{ele} of the ROT-microchip used here was obtained as 0.0566 pF. For the peak voltages, V_P, of the nQDEP signals of 1.5 and 2 Vp, the charges, Q in Eq. (S1), induced on the each electrodes were calculated as 1.2×10^{-13} C and 1.6×10^{-13} C, respectively.

Appendix C: Electrorotation
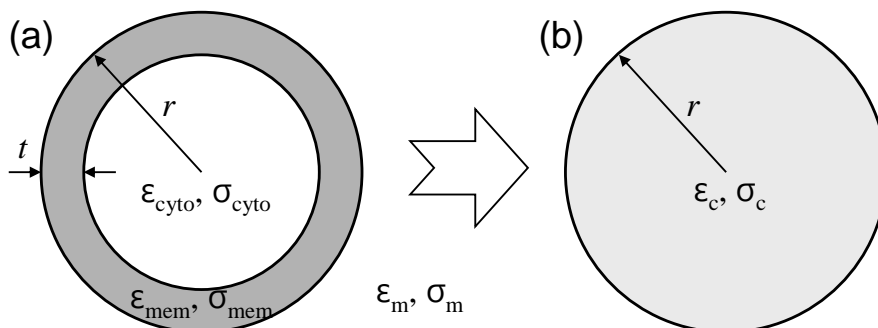
Fig. S3 (a) The single-shell dielectric model and (b) the equivalent homogeneous sphere model for a single cell.

If a single-shell dielectric model (Fig. S3a) is modified as an equivalent homogeneous sphere (Fig. S3b), the effective complex permittivity, $\tilde{\varepsilon}_c = \varepsilon_c - j(\sigma_c/\omega)$, of the equivalent homogeneous sphere can be expressed as:[2]

$$\tilde{\varepsilon}_c = \tilde{\varepsilon}_{mem} \left[\frac{\left(\dfrac{r}{r-t}\right)^3 + 2\left(\dfrac{\tilde{\varepsilon}_{cyto} - \tilde{\varepsilon}_{mem}}{\tilde{\varepsilon}_{cyto} + 2\tilde{\varepsilon}_{mem}}\right)}{\left(\dfrac{r}{r-t}\right)^3 - \left(\dfrac{\tilde{\varepsilon}_{cyto} - \tilde{\varepsilon}_{mem}}{\tilde{\varepsilon}_{cyto} + 2\tilde{\varepsilon}_{mem}}\right)} \right] \tag{S2}$$

where r and t are the outer radius and the membrane thickness of the single-shell dielectric model, respectively. $\tilde{\varepsilon}_{cyto} \left[= \varepsilon_{cyto} - j(\sigma_{cyto}/\omega)\right]$ and $\tilde{\varepsilon}_{mem} \left[= \varepsilon_{mem} - j(\sigma_{mem}/\omega)\right]$ are the complex permittivities of the cytoplasm and membrane of the single-shell dielectric model, respectively.

For the equivalent homogeneous sphere, the imaginary part of the Clausius–Mossotti factor is[3]

$$\mathrm{Im}\!\left[\tilde{f}_{CM}\right] = \frac{\left[\left(\dfrac{\varepsilon_c - \varepsilon_m}{\varepsilon_c + 2\varepsilon_m}\right) - \left(\dfrac{\sigma_c - \sigma_m}{\sigma_c + 2\sigma_m}\right)\right]\omega\tau_{mw}}{1 + \omega^2 \tau_{mw}^2}, \text{ where } \tau_{mw} = \left(\dfrac{\varepsilon_c + 2\varepsilon_m}{\sigma_c + 2\sigma_m}\right), \tag{S3}$$

ε_m and σ_m are the permittivity and conductivity of medium, respectively. The area-specific membrane capacitance, $C_{mem}\left(=\varepsilon_{mem}/t\right)$, and cytoplasm conductivity, σ_{cyto}, can be extracted by minimization of the root mean square error between the measured ROT spectrum and the imaginary part of the Clausius–Mossotti factor in Eq. (S3).

Appendix D: Purity of leukocyte subpopulations
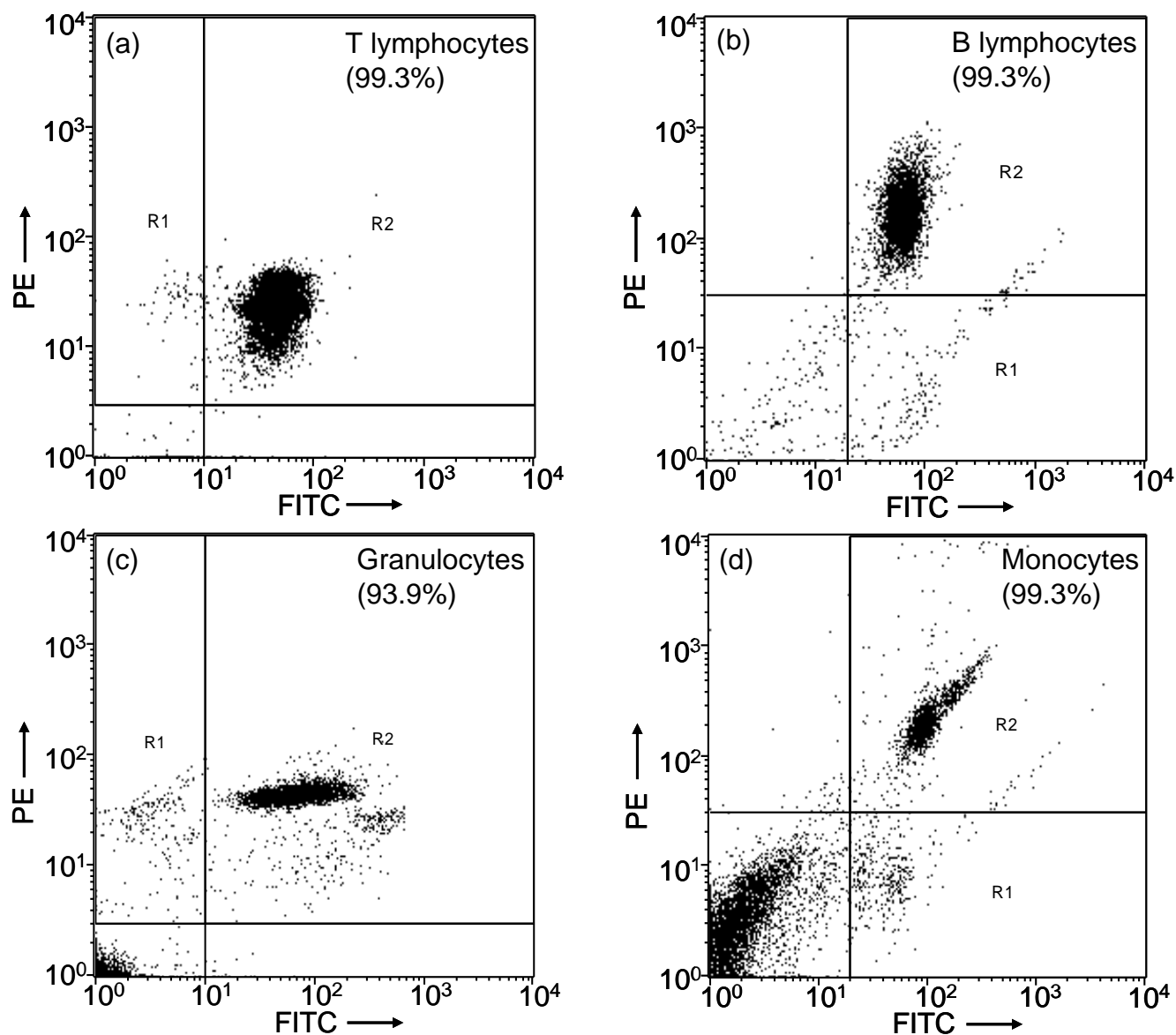
Fig. S4 FACS scatter plots showing fluorescently labeled (a) T lymphocytes with anti-CD3-FITC and red fluorescent nucleic acid stain, (b) B lymphocytes with anti-CD20-PE and anti-CD45-FITC, (c) granulocytes with anti-CD66b-FITC and red fluorescent nucleic acid stain, and (d) monocytes with anti-CD14-PE and anti-CD45-FITC.

Appendix E: Theoretical analysis of the vertical force acting on cells

according to the levitation height
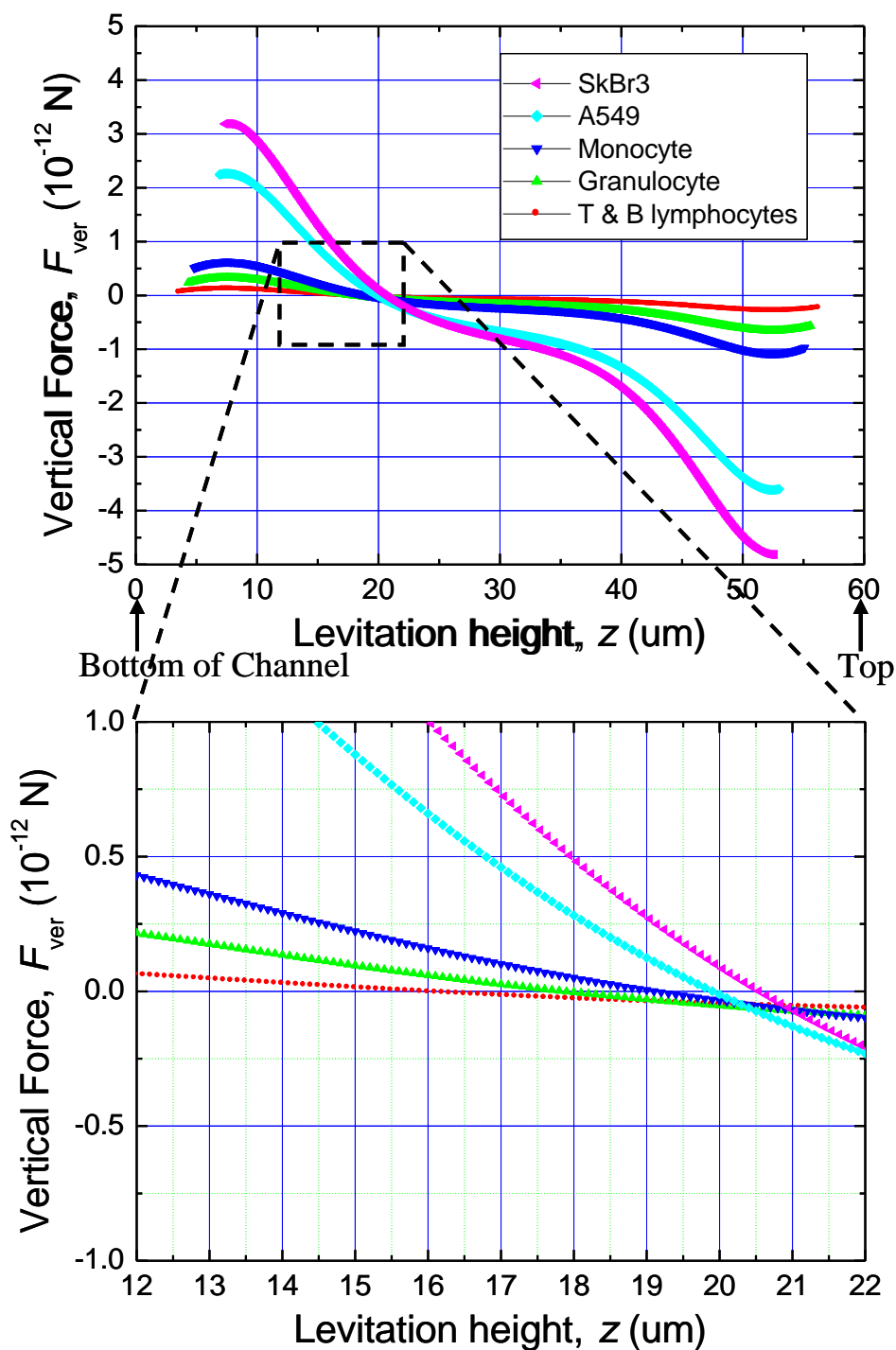
Fig. S5 Theoretical analysis of the vertical force acting on cells [Eq. (5)], which is the sum of the nQDEP forces generated from the top and bottom quadrupole electrodes and the gravitation force, for varying levitation heights along the central axis of the 3D octode.

7

nQDEP signals of 20 kHz, 2 V peak and 1.5 V peak were applied to normal leukocytes and cancer cells, respectively. For the ROT-microchip with a microchannel 60 μm in height, theoretical analysis showed that the cells suspended in 32.6 mS m^{-1} low-conductivity medium were levitated to a height of approximately 15–21 μm. The gravitation force then pulls the cells down to approximately 9–15 μm from the middle of the microchannel.

Appendix F: Theoretical analysis of the levitation heights of cells according to the peak voltage of the nQDEP signal
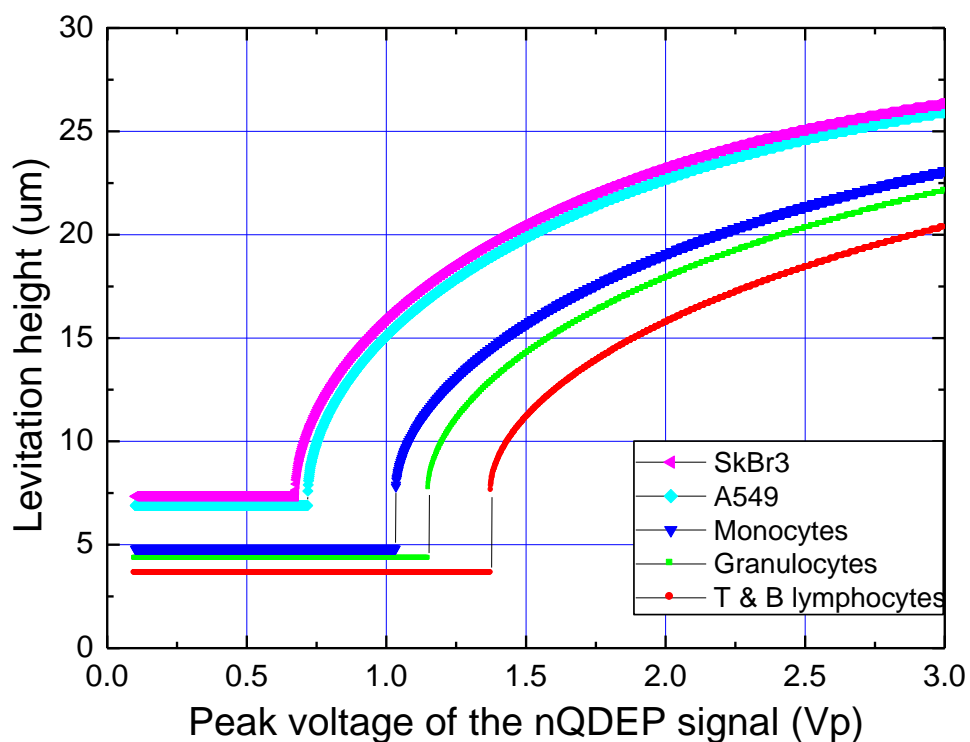
Fig. S6 Analyzed levitation heights of cells according to the peak voltage of the nQDEP signal of 20 kHz. Conductivity of the medium was 32.6 mS m^{-1} and the microchannel height of the ROT-microchip was 60 μm.

Appendix G: Rotation speed of a trapped T lymphocyte for 6 min
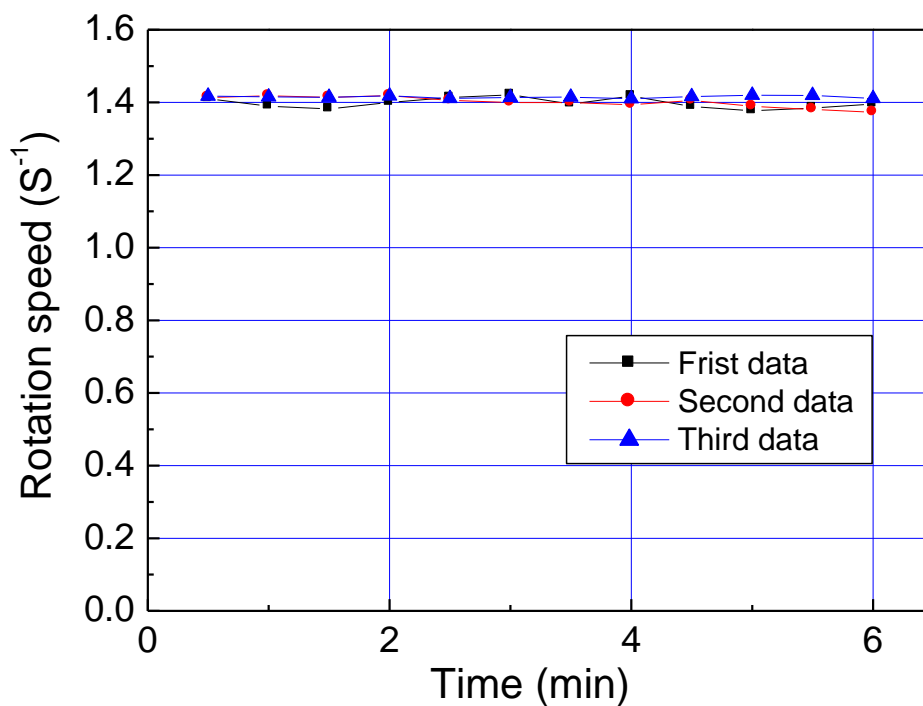
Fig. S7 Rotation speed of a trapped T lymphocyte for 6 min. The T lymphocyte was trapped

by a 20 kHz, 2 Vp nQDEP signal and rotated by a 100 kHz, 0.4 Vp ROT signal.

Reference

1.   J. Z. Chen, A. A. Darhuber, S. M. Troian and S. Wagner, *Lab on a Chip*, 2004, **4**, 473-

      480.

2.   T. B. Jones, *Electromechanics of Particles*, Cambridge University Press, 1995.

3.   T. Sun and H. Morgan, *Microfluidics and Nanofluidics*, 2010, **8**, 423-443.